Proceeding of the 2004 American Control Conference
Boston, Massachusetts June 30 - July 2, 2004

Adaptive Robust Control of an F-15 Aircraft

James Fisher S. Craig Smith John Burken

***Abstract*— Adaptive Robust Control (ARC) is implemented in conjunction with dynamic inversion to control the response of the F-15 IFCS aircraft. Adaptive Robust Control as described by Yao [1] combines the ability of adaptive control to deal with uncertainty in model parameters with the ability of sliding mode control to deal with exogenous disturbances and other uncertainties. Pilot inputs are translated to roll, pitch, and yaw rate commands. The nonlinear dynamic inversion (DI) control law decouples the system to allow tracking of these commands. ARC is implemented in a control loop outside the DI control loop to provide tracking performance in the face of modeling uncertainties and actuator failures. The control is simulated using a full nonlinear 6-DOF simulation of the F-15 IFCS aircraft.**

I. Introduction

This paper describes the application of an adaptive robust controller (ARC) to aircraft flight control. The control action is based upon an uncertain model of aircraft behavior. The assumed nature of the uncertainties is what guides controller design. For our purposes, the uncertainty is grouped into two broad classes: 1) slowly varying with known functional form (variations in the aerodynamic coefficients), 2) quickly varying with unknown functional form. For the purposes of this paper, the first type of uncertainty will be refered to as “parametric” and the second refered to as “unstructured”.

Ultimately the effectiveness of aircraft control is evaluated by a human operator. This makes it difficult to judge performance solely based on numerical responses. While flying qualities can be related to frequency and damping requirements at various flight conditions, there remains a certain amount of subjectivity in the judgement of the response of the system. In this paper, a dynamic inversion control is implemented as an inner loop with Adaptive Robust Control as an outer loop [1]. This is similar to the neural network approaches such as the one described in [2]. The purpose of this controller structure is to decouple the axes of the system in the presence of modeling uncertainties and/or actuator failures in a way that is desirable for the pilot. The failure mode considered in this paper is a stuck control surface. It is important to note that with this form of implementation much of the work required to acheive certain flying qualities is done in creating a reference model. The reference model can be any dynamic system whose response exhibits the desired flying qualities. The work of the dynamic inversion (DI) and the robustifying outer loop is to ensure that the system adequately tracks this reference model.

Adaptive control techniques seek to utilize the assumed structure of equations of motion by dealing with uncertainties in model parameters. If these parameters are slowly varying or do not change at all then adaptive control can have great success. However, in the presence of uncertainty that lies outside of the assumed structure of the models or in the case of rapidly changing parameters, there is no guarantee that the system will behave as the pilot wishes, or that it will even remain stable (with stability being defined as the convergence of the system output to the reference input) [3], [1]. Beyond this, there is no guarantee on the speed of this convergence. It has been shown that if persistence of excitation conditions are not satisfied, the control can be very sensitive to disturbances.

The ability of sliding mode control (SMC) to deal with parametric and unstructured uncertainty while guaranteeing tracking performance makes it very desirable for flight control applications. In addition, it does not require any type of fault detection or explicit control reconfiguration [4], [5]. To achieve perfect tracking, SMC relies on an infinitely fast switching control which when approximated in practical implementations can lead to chattering. While this is well known and has been dealt with in a variety of ways, tracking error is usually only guaranteed to be in some boundary layer region [1], [3], [6], [4]. Sliding mode control and in particular the continuous approximation (a $\mathrm{sat}(\cdot)$ function used in place of the $\mathrm{sgn}(\cdot)$ function) can be thought of as very high gain control. In aircraft problems this leads to rate/position saturation of the actuators which can result in instability. Several authors have investigated means to preserve stability in the presence of of rate/position saturation [4], [5]. The problem of rate/position limits is not specifically addressed in this paper, though included in simulation model.

Adaptive Robust Control (ARC) as described by Yao in [1] provides a bridge between the two methods described above. The control consists of a sliding mode portion which ensures stability as well as performance (in the form of a time constant to the sliding surface) coupled with an adaptive portion which can “learn” the parametric uncertainty present in the system. In this way, the control can handle the unstructured uncertainties and provide steady state tracking performance. The control is implemented on the full nonlinear 6-DOF simulation of the F-15 IFCS.

email: mzungu@tamu.edu This material is based upon work supported by NASA under NGT4-52435. Any opinions, findings, and conclusions or recommendations expressed in this publication are those of the authors and do not necessarily reflect the views of NASA
email: craig_smith@maxtor.com Maxtor Corporation, Milpitas CA
email: john.burken@dfrc.nasa.gov NASA Dryden Flight Research Center

II. NOTATION

The following notation will be used throughout this paper. The nomenclature for aircraft parameters is fairly standard and is adopted from [7]:

p, q, r	roll, pitch, and yaw rates of an aircraft
δ_a, δ_e, δ_r	Synthetic surface position commands
α	angle of attack
β	sideslip angle
PI	pilot inputs
$F(s)$	precompensator: converts PI to p, q, r cmds
sgn(x)	sign of x
sat(x)	sat$(x) : \mathbb{R}^n \mapsto [-1, 1]$

III. SUMMARY OF ARC AS PRESENTED BY YAO [1]

The motivation for using Adaptive Robust Control in a particular application is to achieve a combination of the transient performance and robustness of sliding mode control with the steady state error guarantees of adaptive control. As a simple example, consider a scalar dynamic system with state x and input ν described by the following differential equation:

$$\dot{x} = \theta\varphi(x,t) + \nu + \Delta(x,t,u), \quad x \in \mathbb{R}, \theta \in \mathbb{R}^{1\times p} \tag{1}$$

The variable θ represents a vector of unknown parameters, $(\theta_1, \ldots, \theta_p)$. The effect of each θ_i on the derivatives of the state is a known function of the state and time, $\varphi_i(x,t)$. Unstructured uncertainty, denoted $\Delta(x,t,u)$, may be functionally dependent on time, the state, x, and/or the input. This allows $\Delta(x,t,u)$ to capture the effects of both exogenous disturbances and unknown dynamics. The values of θ and $\Delta(x,t,u)$ are not known, but are assumed to have known bounds.

$$\begin{aligned} \theta_i \in \Omega_{\theta_i} &\triangleq \Big\{\theta_i : \theta_{i,min} < \theta_i < \theta_{i,max}\Big\} \\ |\Delta(x,t,u)| &\leq \delta(x,t), \quad i = 1 \ldots p \end{aligned} \tag{2}$$

The function $\delta(x,t)$ is bounded with respect to time such that $\delta(x(t),t) \in \mathcal{L}_\infty$ whenever $x(t) \in \mathcal{L}_\infty$.

The output variable (x) should track a reference $x_d(t)$. Define the tracking error, $e = x(t) - x_d(t)$. The SMC portion of the control will be based upon a filtered tracking error. Auxillary variables x_c, z, y_c, and x_r are defined as follows ($x_c \triangleq$ filter states, $x_r \triangleq$ filtered reference, $z \triangleq$filtered error):

$$\begin{aligned} \dot{x}_c &= A_c x_c + B_c e & x_c \in \mathbb{R}^{n_c}, A_c \in \mathbb{R}^{n_c \times n_c}, \\ z &= C_c x_c + e = y_c + e & B_c \in \mathbb{R}^{n_c}, C_c \in \mathbb{R}^{1\times n_c} \\ &= x - x_r & x_r \triangleq x_d(t) - y_c \end{aligned} \tag{3}$$

The system given by (A_c, B_c, C_c) is a filter for the tracking error. The sliding surface associated with the SMC portion of the control is described by $z = 0$. The dynamics on the sliding surface are designed using (A_c, B_c, C_c). The transfer function from e to z has relative degree zero. The term x_r is a filtered version of the command x_d.

The adaptive robust control law which ensures the convergence of the system given by Equation (1) to the sliding surface $(z = 0)$ is given below.

$$\nu = \nu_s + \nu_a \tag{4}$$

$$\nu_a = \dot{x}_r - \hat{\theta}_\pi \varphi(x,t) \tag{5}$$

$$\nu_s = -kz - \mu\Big(h(x,t), z\Big) \tag{6}$$

$$\dot{\hat{\theta}} = z\varphi(x,t)^T \gamma \tag{7}$$

The ν_s portion of the control can be thought of as the sliding mode portion, providing stability in the face of disturbances and transient performance guarantees (through selection of k) [1]. The ν_a term is the adaptive portion of the control law. It consists of an approximate inversion of the dynamics $(\hat{\theta}_\pi \varphi(x,t))$ as well as feedforward control, $\dot{x}_r$. If $\hat{\theta}_\pi$ is replaced with a nominal approximation or best guess for θ, SMC is recoverd.

The vector $\theta_\pi = (\theta_{\pi 1}, \ldots, \theta_{\pi p})$. The $(\cdot)_{\pi i}$ function denotes a projection mapping of a variable onto Ω_{θ_i}. One possible implementation is the following.

$$\theta_{\pi i} = \begin{cases} \theta & \theta \in \Omega_{\theta_i} \\ \theta_{i,max} & \theta > \theta_{i,max} \\ \theta_{i,min} & \theta < \theta_{i,min} \end{cases} \tag{8}$$

The function $\mu\Big(h(x,t), z\Big)$ is the effective sliding mode portion of the control. If $\mu(h,z) = h(x,t)\text{sgn}(z)$, one is assuming infinitely fast switching and a discontinous control law (standard SMC). A continuous approximation is made for the signum function, resulting in $\mu(h,z) = h(x,t)\text{sat}(z/\varepsilon)$. The following is a sufficient condition to guarantee convergence to the sliding surface (or a boundary layer in the case of $\mu(h,z) = h(x,t)\text{sat}(z/\varepsilon)$).

$$|h(x,t)| \geq \left|\Big(\theta - \hat{\theta}_\pi\Big)\varphi(x,t) + \Delta(x,t,u)\right| \tag{9}$$

The γ term in equation (4) is a positive constant (or if $\varphi(x,t)$ is a vector, it is a diagonal positive definite matrix). Proof of stability for this control law can be found in [1] (as the proof to Theorem 4 in Chapter 2).

IV. WHY USE ARC INSTEAD OF SMC?

In flight control applications of SMC it is common to include an integrator as part of the sliding surface [6], [4], [5], [8], [9], [10]. The objective of this inclusion is to deal with steady state errors. SMC regulates the filtered error response $(z \to 0)$. The stability of the linear differential equation governing the sliding surface requires that every term that makes up the surface must decay to zero when $z = 0$. If an integrator is included as part of the surface and the SMC forces the system onto the sliding surface, the integral of the error must go to zero as $t \to \infty$. In essence, the control variable becomes the integral of the error instead of tracking error. On face, this does not sound out of the ordinary. However, if the dynamics of the system were to suddenly change resulting in a positive integral of the error, the system must undershoot by the same amount to allow the sliding surface to decay to zero. If a saturation function is used, removing steady state error is accomplished by maintaining a steady-state z value.

Using a signum function, there is an obvious difference between ARC and SMC. With a saturation function, it might seem that these control laws would be equivalent to one another. This is not the case. As an example, consider the following dynamic system:

$$\begin{aligned} \dot{x} &= d(t) + \nu \\ |d(t)| &\leq D \end{aligned} \tag{10}$$

The objective is to regulate the state, ($x \rightarrow 0$). The magnitude of the disturbance, $d(t)$, is bounded by D. The continous approximation of SMC with an integrator included as part of the sliding surface has the following form:

$$\begin{aligned} \nu_1 &= -k_1 z_1 - D_1 \text{sat}(z_1/\varepsilon) \\ z_1 &= x(t) + \lambda \int_0^t x(t)dt \end{aligned} \tag{11}$$

When the saturation operates in the linear region the above control law becomes:

$$\nu_1 = -\left(k_1 + D_1/\varepsilon + \lambda\right) x - \left(k_1 + D_1/\varepsilon\right) \lambda \int_0^t x dt \tag{12}$$

When the saturation function reaches its upper limit the SMC law becomes the following:

$$\nu_1 = -\left(k_1 + \lambda\right) x - k_1 \lambda \int_0^t x dt - D_1 \tag{13}$$

The ARC control law with continuous approximation is given by the following (d is modeled with a $\hat{\theta}$):

$$\begin{aligned} \nu_2 &= -k_2 z_2 - D_2 \text{sat}(z_2/\varepsilon) - \hat{\theta}_\pi \\ z_2 &= x(t) \\ \dot{\hat{\theta}} &= \gamma z_2 = \gamma x \end{aligned} \tag{14}$$

When the saturation operates in the linear region, and $\hat{\theta}_\pi$ is not saturated:

$$\nu_2 = -\left(k_2 + D_2/\varepsilon\right) x - \gamma \int_0^t x(t)dt \tag{15}$$

If the saturation function is at its upper limit, but $\hat{\theta}_\pi$ has not reached a limit:

$$\nu_2 = -k_2 x - \gamma \int_0^t x(t)dt - D_2 \tag{16}$$

In both control laws, when operating in the linear region of the saturation function, the result is porportional-integral control. Using Equations (12) and (15) gains can be selected that make the control laws equivalent for this case. Upon reaching a saturation limit, the gains that the two control laws equivalent do not make Equations (13) and (16) equivalent. There are three major differences between ARC and SMC. First, the integral gain for ν_1 changes when $|z| > \varepsilon$, but does not change for ν_2. Second, $\hat{\theta}_\pi$ can be saturated meaning the integral portion of ν_2 becomes zero. The integral portion of ν_1 may reduce gain but is otherwise unbounded. Third, if more is known about the model, these parameters can be included in the ARC law. This is not possible with SMC.

ARC is proposed as a means to utilize the transient performance of sliding mode control and its abilities to reject disturbances. ARC can also account for the the steady state errors and the slowly varying dynamics without the drawback of including an integral as a part of the sliding surface. This allows the system to achieve the sliding surface ($z \rightarrow 0$) even when using a saturation function in the SMC portion of the control law.

V. Pitch Example

A dynamic model for an aircraft can be put into the form described in Section III. A block diagram showing how the control would be implemented on the pitch axis is given in Figure 1. Linear dynamic models are considered for simplicity in this section. For small variations around a single flight condition, the pitch dynamics of an aircraft can be modeled by the following.

$$\begin{bmatrix} \dot{u} \\ \dot{\alpha} \\ \dot{q} \end{bmatrix} = A_q \begin{bmatrix} u \\ \alpha \\ q \end{bmatrix} + B_q \delta_e \qquad y = C_q \begin{bmatrix} u \\ \alpha \\ q \end{bmatrix} = q \tag{17}$$

It is assumed that there is a one dimensional synthetic control, δ_e, which will be allocated to the pitch actuators (for the F-15 IFCS aircraft it is the stabilators only). The stick input is considered as the source of a pitch rate command.

A dynamic inversion control (with respect to the dynamics of q) applied to the system with dynamics given by Equation (17), results in the following closed loop.

$$\dot{q} = C_q \left(A_q - B_q P^\dagger C_q \hat{A}_q \right) \begin{bmatrix} u \\ \alpha \\ q \end{bmatrix} + C_q B_q P^\dagger \dot{q}_{des} \tag{18}$$

In the above expression, $\hat{B}_q$, $\hat{A}_q$ are the nominal values of B_q and A_q respectively. The variable P represents $C_q \hat{B}_q$. The $(\cdot)^\dagger$ function is used to represent a generalized inverse. If the plant is modeled perfectly ($\hat{B}_q = B_q$ and $\hat{A}_q = A_q$), $\dot{q} = \dot{q}_{des}$.

This will not be the case in the presence of either modeling errors or disturbances. Modeling errors ($A_q \neq \hat{A}_q$, $B_q \neq \hat{B}_q$, etc.) result in governing (closed loop) equations of the form:

$$\dot{q} = \theta_u u + \theta_\alpha \alpha + \theta_q q + \theta_{\dot{q}_{des}} \dot{q}_{des} \tag{19}$$

where θ_u, θ_α, θ_q, and $\theta_{\dot{q}_{des}}$ depend on the modeling errors. If the aircraft were to experience an actuator failure where an actuator became unresponsive we might model the closed loop as the following.

$$\dot{q} = \theta_u u + \theta_\alpha \alpha + \theta_q q + \theta_{\dot{q}_{des}} \dot{q}_{des} + \Delta(t) \tag{20}$$

In flight, variations in q are much larger than those of α or u. Additionally, in the face of a constant exogenous disturbance such as a stuck control surface, we will have a new equilibrium point in terms of our uncontrolled states α and u. Define the new trim points as α_t and u_t. Let $\tilde{\alpha} = \alpha - \alpha_t$ and $\tilde{u} = u - u_t$. Now define

$$\theta_u u + \theta_\alpha \alpha = \theta_c + \theta_u \tilde{u} + \theta_\alpha \tilde{\alpha} \tag{21}$$

Where $\theta_c = \theta_u u_t + \theta_\alpha \alpha_t$. This allows us to model the unknown constant perturbation as part of our shape function. The $\theta_u \tilde{u}$ and $\theta_\alpha \tilde{\alpha}$ terms can be used to capture the perturbations from the new trim. The dynamics can be expressed as follows:

$$\begin{aligned} \dot{q} &= \theta_q q + \theta_c + \theta_u \tilde{u} + \theta_\alpha \tilde{\alpha} + \theta_{\dot{q}_{des}} \dot{q}_{des} + \Delta(t) \\ &= \theta_q q + \theta_c + \dot{q}_{des} + \Delta\left(t, \dot{q}_{des}, \tilde{\alpha}, \tilde{u}\right) \end{aligned} \tag{22}$$

The shape function (denoted as $\varphi(x,t)$ in Equation (1)) for the pitch dynamics is $\left[\begin{array}{cc} q & 1 \end{array}\right]^T$. If desired, the θ_q term can be treated as part of the disturbance Δ as well. This would turn the adaptive portion of the control into pure integral control. In this manner, we are allowed to include an integral control without having it as part of the sliding mode. This gives the benefit of removing steady state error without the drawback of forcing our primary control variable to be the integral of the error.

VI. 6-DOF RESULTS

A. Dynamic Inversion

The dynamics of an aircraft can be represented by

$$\dot{x} = A(x,y) + B(x,y)\,\delta \tag{23}$$

where $x = [p,q,r]^T$, y is made up of all the all other flight condition variables and aircraft parameters, and $\delta = [\delta_a, \delta_e, \delta_r]^T$. This is a generalization of the full dynamic equations of motion for the body axis rates as given in [7]. The terms in Equation (23) can be used to invert the dynamics and "replace" them with the desired dynamics (see Figure 2). Figure 2 shows a block diagram of this implementation. The precompensator, or $F(s)$, takes pilot stick commands and converts them to $\dot{p}$, $\dot{q}$, and $\dot{r}$ reference signals. The objective of the DI inner loop is to control the values of p, q, and r. The controls come in the form of the δ vector which are synthetic control commands for roll, pitch, and yaw. These synthetic controls are then allocated to the actuators. In our example, this is done through a static control allocation of the form.

$$\bar{\delta} = T\delta \tag{24}$$

The actual surface commands are the elements of the $\bar{\delta}$ vector. The control allocation (be it static or dynamic) must be included as part of $B(x,y)$. $B(x,y) \in \mathbb{R}^{3\times 3}$ is invertible. The dynamic inversion control law takes the form

$$\delta_{des} = B(x,y)^{-1}\left(\dot{x}_{des} - A(x,y)\right) \tag{25}$$

where $\dot{x}_{des} = [\dot{p}_{des}, \dot{q}_{des}, \dot{r}_{des}]^T$.

B. ARC Implementation

The objective of the dynamic inversion control law is to decouple the p, q, and r axes. This means it is desired for our system to be diagonal (when linearized) and that any off diagonal terms can be treated as perturbations. As a result three independent loops are utilized (one for each axis). Figure 2 depicts a block diagram of this control implementation. For each axis (roll, pitch, yaw) the control law presented in Equation (4) is used. For this example, the shape function ($\varphi(x,t)$) used is a constant, 1. In addition, a continuous approximation to SMC is used. The sliding mode portion of the control is set as $\mu\left(h\left(x,t\right), \mathrm{sgn}(z)\right) = h(x,t) sat\left(\frac{z}{\varepsilon}\right)$, where ε is a positive constant and $h(x,t)$ obeys Equation (9). The ARC control is of the following form:

$$\begin{aligned} \dot{p}_{com} &= \dot{p}_r - \hat{\theta}_{\pi,p} - k_p z_p - h_p sat\left(z_p/\varepsilon\right) \\ \dot{q}_{com} &= \dot{q}_r - \hat{\theta}_{\pi,q} - k_q z_q - h_q sat\left(z_q/\varepsilon\right) \\ \dot{r}_{com} &= \dot{r}_r - \hat{\theta}_{\pi,r} - k_r z_r - h_r sat\left(z_r/\varepsilon\right) \end{aligned} \tag{26}$$

C. Numerical Results

Presented here are simulated F-15 IFCS aircraft responses both before and after failures occur. A reference model that describes desirable flying qualities and converts pilot inputs to p, q, and r reference signals is given. The performance of the control scheme is evaluated in terms of its ability to track the reference signal. The ARC ensures the robustness of the dynamic inversion control law to modeling uncertainties and/or failures. The data presented here is at Mach 0.75, 20,000ft. In the course of flight a stabilator failure occurs at 8.5 seconds. The stabilator fails to 50% of its maximum positive value and remains here for rest of the simulation. There is also mismatch between the simulated model and the model used for the DI. Rate limits as well as position limits are included in the model, though not explicitly addressed by the ARC.

Figures 3 and 4 give the roll and pitch responses of the aircraft respectively. The yaw response of the aircraft is not shown here for space reasons, but closely resembles that of Figure 3. Due to security issues the data presented in the paper will be scaled by its maximum value. The reference signals are selected to excite each axis both independently and in conjuction with one another. This sequence of synthesized references is designed to exhibit coupling in the axes. This is important from a pilot standpoint because it is undesirable to attempt a pitch maneuver and get a large amount of roll or yaw. The references were also chosen because they are fairly aggressive. At first glance, the tracking results do not seem to be as good as one might hope. However, it is the goal of this paper to push the limits of the system. The inputs are rapidly varying and excite all axes simultaneously. These results are indicative of the response over the entire flight envelope.

Stabilator failures have the largest effect on the response of the pitch axis. Only two actuators control the pitch response, the left and right stabilators. The two stabilators are also used in roll control. The result is a very large induced roll to pitch coupling. The objective of the control scheme is to account for this coupling without any "knowledge" of its existence. Upon examination of Figure 3 we see that there is little coupling in the roll axis due to pitch commands. For example, at about 14 seconds, there is a large pitch input, but the roll command tracks its reference closely. The same holds true for the yaw response (although not shown here). In the pitch response (Figure 4), we see pitch errors as a result of roll command after the failure. This is evident at t =15s in Figure 4. This is because the commanded maneuvers are aggressive enough to reach actuator rate limits consistently.

These figures also demonstrate the transient response of the aircraft to the failure. The simulated pilot does nothing to bring the aircraft under control. In this sense, the aircraft should be "hands-off" stable at the occurance of a failure. Figures 5 and 6 show the tracking error responses of the system. For roll and yaw (Figure 5), the error just after the time of failure ($t = 8.5$) is of the same magnitude as the time previous to the error. The sudden introduction of a failure into the system has a small impact on the tracking error. The impact on the pitch axis is larger. The result is a lag-like behavior that occurs after a failure (see Figure 4).

Figure 7 shows the stabilator responses for the simulation. At the time of failure (8.5 seconds), the right stabilator moves to its failure position and sticks. This leaves only one pitch actuator to both deal with the steady state pitch moment and to track pitch commands. The stuck stabilator also induces a constant roll rate disturbance. This is countered both by the ailerons and the other stabilator. Figure 8 shows the left aileron response of the aircraft. The ailerons are used differentially, so the right aileron response is the negative of the left.

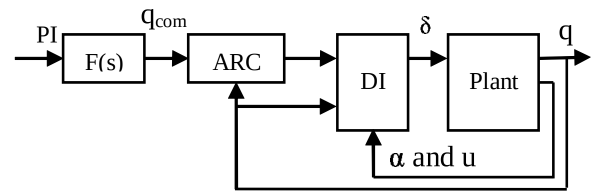

Fig. 1. ARC Implementation on Aircraft Pitch Axis

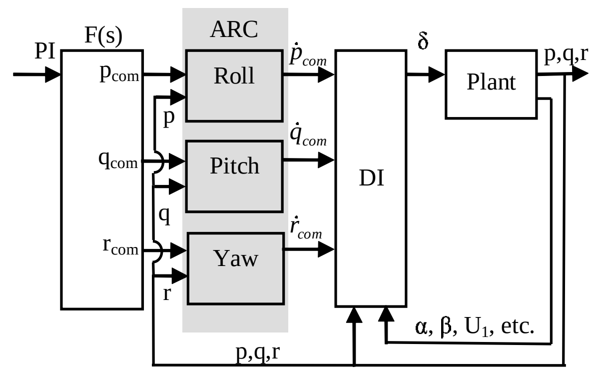

Fig. 2. ARC Implementation on nonlinear Aircraft Dynamics

VII. Conclusion

Adaptive Robust Control is used to control an aircraft in the presence of uncertainty in model parameters and actuator failures. ARC is implemented as an outer loop to a full nonlinear dynamic inversion control law. Pilot commands are converted to desired roll, pitch, and yaw rates which are tracked by the combination of ARC and the dynamic inversion control law. The control maintains good tracking accuracy during fairly aggressive maneuvers in the presence of actuator failures. This is accomplished without requiring any control reconfiguration or failure detection algorithms. Simulation study of the response of a 6-DOF full nonlinear model of the F-15 IFCS under ARC control (with actuator rate and position limits included) allowed trained pilots to acheive performance in the presence of failures that could not be achieved in the absence of this technique.

References

[1] Bin Yao. *Adaptive Robust Control of Nonlinear Systems with Applications to Control of Mechanical Systems.* PhD thesis, University of California at Berekeley, 1996.

[2] Flavio Nardi and Anthony J. Calise. Robust adaptive nonlinear control using single hidden layer neural networks. In *Proceedings of the 39th IEEE Conference on Decision and Control*, pages 3825–3830. IEEE, 2000.

[3] Jean-Jacques E. Slotine and Weiping Li. *Applied Nonlinear Control.* Prentice Hall, New Jersey, 1991.

[4] Y. Shtessel, J. Buffington, M. Pachter, P. Chandler, and S. Banda. Reconfigurable flight control on sliding modes addressing actuator deflection and deflection rate saturation. In *AIAA Guidance, Navigation, and Control Conference and Exhibit*, pages 127–137. AIAA, 1998.

[5] Y. Shtessel, J. Buffington, and S. Banda. Multiple time scale flight control using re-configurable sliding modes. In *Proceedings of the 37th IEEE Conference on Decision and Control*, pages 4196–4201. IEEE, 1998.

[6] R.A. Hess and S.R. Wells. Sliding mode control applied to reconfigurable flight control design. *Journal of Guidance, Control, and Dynamics*, 26(3), 2003.

[7] Bernard Etkin. *Dynamics of Flight, Stability, and Control.* John Wiley and Sons, New York, 2nd edition, 1982.

[8] Yuri Shtessel, James Buffington, and Siva Banda. Tailless aircraft flight control using multiple time scale reconfigurable sliding modes. *IEEE Transactions on Control Systems Technology*, 10(2):288–296, 1998.

[9] R.A. Hess and S.R. Wells. Multi-input/multi-output sliding mode control for a tailless fighter aircraft. *Journal of Guidance, Control, and Dynamics*, 26(3), 2003.

[10] S.R. Wells and R.A. Hess. Mimo sliding mode control for a tailless fighter aircraft, an alternative to reconfigurable architectures. In *AIAA Guidance, Navigation, and Control Conference and Exhibit*, pages 1–13. AIAA, 1998.

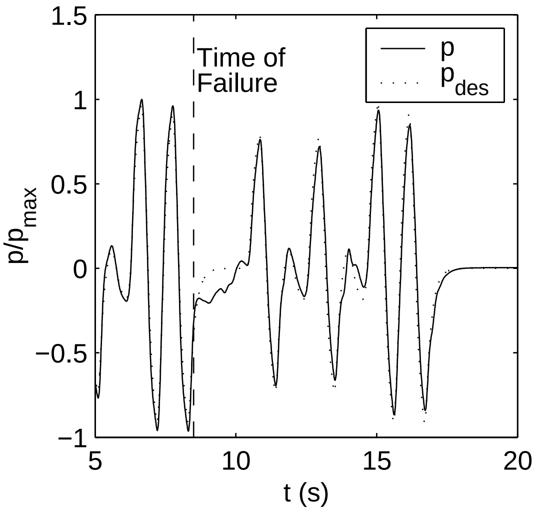

Fig. 3. Roll response of aircraft

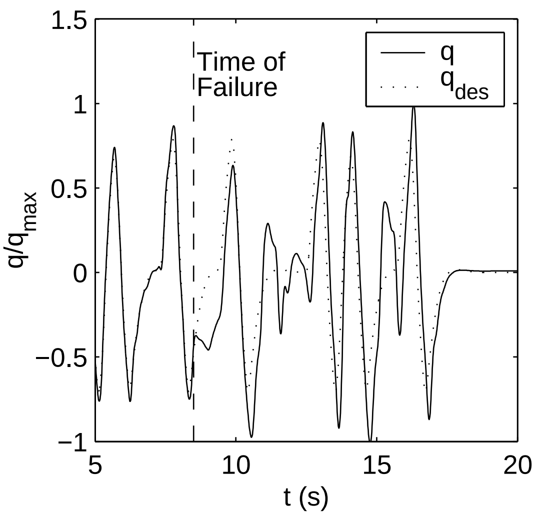

Fig. 4. Pitch response of aircraft

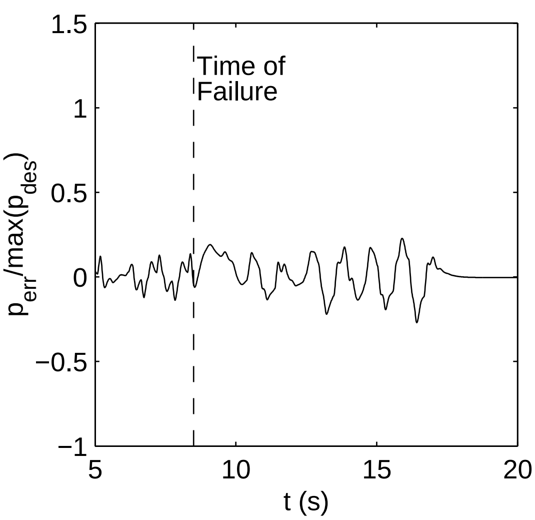

Fig. 5. Roll error response

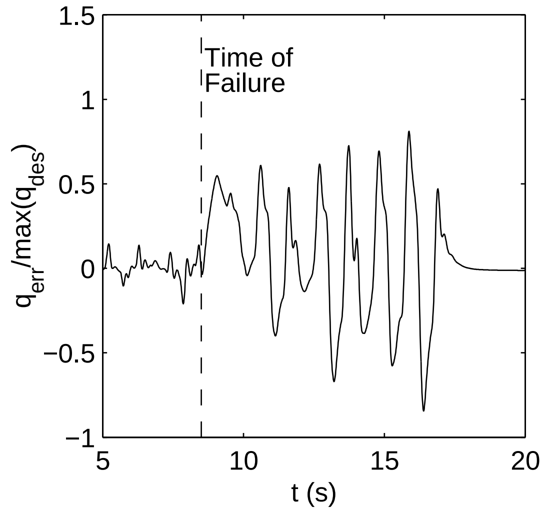

Fig. 6. Pitch error response

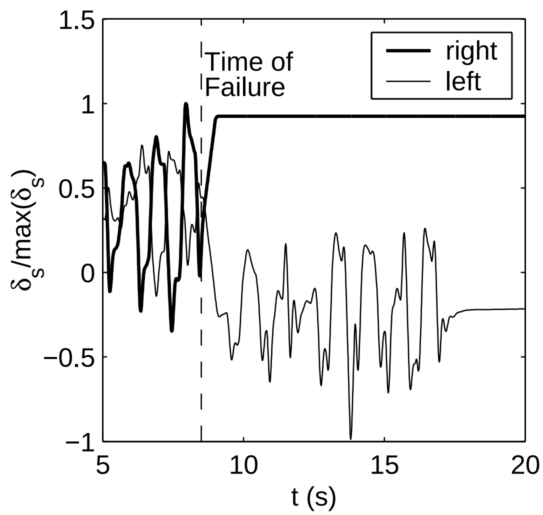

Fig. 7. Stabilator responses

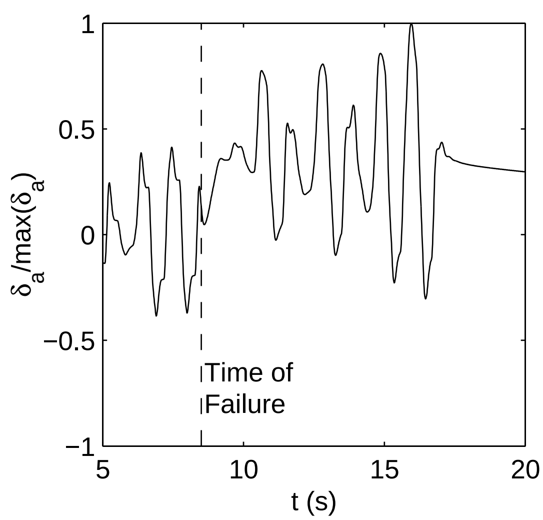

Fig. 8. Left Aileron response